Surface-site-selective study of valence electronic states of a clean Si(111)-7×7 surface using Si $L_{23}VV$ Auger electron and Si 2p photoelectron coincidence measurements

Takuhiro Kakiuchi,[1] Masashi Tahara,[1] Shogo Hashimoto,[2] Narihiko Fujita,[2] Masatoshi Tanaka,[2] Kazuhiko Mase,[3,4] and Shin-ichi Nagaoka[1]

[1]*Department of Chemistry, Faculty of Science, Ehime University, 2-5 Bunkyo-cho, Matsuyama 790-8577, Japan*
[2]*Department of Physics, Faculty of Engineering, Yokohama National University, 79-5 Tokiwadai, Hodogaya-ku, Yokohama 240-8501, Japan*
[3]*Institute of Materials Structure Science, Japan's National Laboratory for High Energy Physics (KEK), 1-1 Oho, Tsukuba 305-0801, Japan*
[4]*The Graduate University for Advanced Studies, 1-1 Oho, Tsukuba 305-0801, Japan*

(Received 10 September 2010; revised manuscript received 3 December 2010; published 24 January 2011)

Valence electronic states of a clean Si(111)-7×7 surface are investigated in a surface-site-selective way using high-resolution coincidence measurements of Si $L_{23}VV$ Auger electrons and Si 2p photoelectrons. The Si $L_{23}VV$ Auger electron spectra measured in coincidence with energy-selected Si 2p photoelectrons show that the valence band at the highest density of states in the vicinity of the rest atoms is shifted by ∼0.95 eV toward the Fermi level (E_F) relative to that in the vicinity of the pedestal atoms (atoms directly bonded to the adatoms). The valence-band maximum in the vicinity of the rest atoms, on the other hand, is shown to be shifted by ∼0.53 eV toward E_F relative to that in the vicinity of the pedestal atoms. The Si 2p photoelectron spectra of Si(111)-7×7 measured in coincidence with energy-selected Si $L_{23}VV$ Auger electrons identify the topmost surface components, and suggest that the dimers and the rest atoms are negatively charged while the pedestal atoms are positively charged. Furthermore, the Si 2p–Si $L_{23}VV$ photoelectron Auger coincidence spectroscopy directly verifies that the adatom Si 2p component (usually denoted by C_3) is correlated with the surface state just below E_F (usually denoted by S_1), as has been observed in previous angle-resolved photoelectron spectroscopy studies.

DOI: 10.1103/PhysRevB.83.035320 PACS number(s): 73.20.At, 79.60.−i, 68.35.B−, 82.80.Pv

I. INTRODUCTION

A clean reconstructed Si(111)-7×7 surface is especially attractive for surface-site-selective studies, because the unit cell of the 7×7 structure includes 12 adatoms, six rest atoms, 36 pedestal atoms (atoms directly bonded to the adatoms), 18 dimer atoms, and one corner-hole atom.[1] Actually, Si(111)-7×7 was selected as the first sample for surface-site-resolved charge imaging using scanning tunneling microscopy (STM).[2] Hamers *et al.* obtained real-space images of adatom dangling bond, rest atom dangling bond, and adatom back bond states using current-imaging tunneling spectroscopy (CITS).[3] Since then, local valence electronic states of Si(111)-7×7 have been extensively investigated with CITS and scanning tunneling spectroscopy (STS).[4–7] The charge density and surface structure of Si(111)-7×7 have been studied also with synchrotron radiation core-level photoelectron spectroscopy (SR-CL-PES) in a surface-site-selective way.[8–11] Karlsson *et al.* assigned the main Si 2p surface components, and supported the negative charge transfer from the adatoms to the rest atoms.[8] In this paper, we report on a surface-site-selective study on the valence electronic states of a clean Si(111)-7×7 surface using high-resolution coincidence measurements of Si $L_{23}VV$ Auger electrons and Si 2p photoelectrons.

Auger photoelectron coincidence spectroscopy (APECS) has been widely used to study dynamics induced by core-level excitations of surfaces.[12–15] APECS is more surface sensitive than the conventional SR-CL-PES and Auger electron spectroscopy (AES), because the escape depth (ED) of electrons detected by APECS is given by

$$\frac{1}{\mathrm{ED}_{\mathrm{APECS}}} = \frac{1}{\mu_{\mathrm{Pe}}} + \frac{1}{\mu_{\mathrm{Ae}}}, \qquad \mu_{\mathrm{Pe}} = \lambda_{\mathrm{Pe}} \cos\theta_{\mathrm{Pe}}, \quad \mu_{\mathrm{Ae}} = \lambda_{\mathrm{Ae}} \cos\theta_{\mathrm{Ae}}, \tag{1}$$

where λ and θ denote the inelastic mean free path (IMFP) and the emission angles of the detected electrons, respectively.[13] The subscripts APECS, Pe, and Ae denote electrons detected by APECS, PES, and AES, respectively. Core-valence-valence (CVV) APECS is a unique technique bridging CL-PES and valence electron spectroscopy.[16,17] Very recently, we studied a clean Si(100)-2×1 surface in a surface-site-selective way using high-resolution Si $L_{23}VV$ Auger electron Si 2p photoelectron coincidence spectroscopy (Si $L_{23}VV$–Si 2p APECS), and obtained information on the energy level where the valence-band density of states (DOS) is highest, and the valence-band maximum (VBM) in the vicinity of the Si up-atoms and the Si second layer.[18] In Si $L_{23}VV$–Si 2p APECS, Si 2p photoelectrons with a fixed kinetic energy corresponding to specific sites are detected by an electron energy analyzer, while Auger electrons in the Si $L_{23}VV$ Auger electron region are measured by another analyzer. The intensity of an Si $L_{23}VV$ Auger peak ($I_{L_{23}VV}$) is given by the equation

$$I_{L_{23}VV} \propto \left| \left\langle \phi_{L_{23}} \phi_{\varepsilon} \left| \frac{e^2}{r_{V_1V_2}} \right| \phi_{V_1} \phi_{V_2} \right\rangle \right|^2, \tag{2}$$

where $\phi_{L_{23}}$, ϕ_{ε}, and ϕ_{V_i} ($i = 1,2$) express the wave functions of L_{23}, the Auger electron, and the valence electrons (V_1 and V_2), respectively. $r_{V_1V_2}$ is the distance between the two valence electrons. The interaction potential term $e^2/r_{V_1V_2}$ represents the Coulomb repulsion between the two valence electrons. As the first step of discussing the local valence electronic structures, we assume that the highest peak of the Si $L_{23}VV$–Si 2p APECS reflects the binding energy of the Si valence band at the highest DOS in the vicinity of the associated Si 2p sites, because $e^2/r_{V_1V_2}$ is expected to be largest when the DOS becomes highest.[18] We can also discuss the binding energy of the VBM in the vicinity of a specific Si

surface site based on APECS. The cutoff energy at the high Auger electron kinetic energy side of Si $L_{23}VV$–Si $2p$ APECS corresponds to the VBM at the specific site.[18] Si $L_{23}VV$–Si $2p$ APECS can probe any valence states, but is most suitable for investigations of local surface states because of the short ED_{APECS}. Because Si $2p$ photoelectron peaks of silicon surface sites can be resolved in high-resolution SR-CL-PES,[19,20] Si $L_{23}VV$–Si $2p$ APECS provides information on local valence electronic states in the vicinity of individual surface sites.

Measurements of photoelectrons in coincidence with energy-selected Auger electrons, on the other hand, offer topmost-surface-sensitive CL-PES.[21] This technique is sometimes called photoelectron Auger coincidence spectroscopy (PEACS).[22] Very recently, we measured Si $L_{23}VV$ Auger electron Si $2p$ photoelectron coincidence spectra (Si $2p$–Si $L_{23}VV$ PEACS) of Si(100)-2×1, and identified the topmost-surface Si $2p$ components by taking advantage of the extremely short escape depth of 1.2 Å.[23]

In this paper, we report on the surface-site-selective Si $L_{23}VV$ AES and Si $2p$ PES of clean Si(111)-7×7 measured with Si $L_{23}VV$–Si $2p$ APECS and Si $2p$–Si $L_{23}VV$ PEACS. The Si $L_{23}VV$–Si $2p$ APECS indicated that the valence band in the vicinity of the rest atoms shifted towards the Fermi level (E_F) relative to that of the pedestal atoms. The results are consistent with previous angle-resolved PES,[24,25] CITS,[3] and theoretical studies.[26] With Si $2p$–Si $L_{23}VV$ PEACS, on the other hand, topmost-surface Si $2p$ components are considerably enhanced. The results suggest that the dimers and the rest atoms are negatively charged while the pedestal atoms are positively charged. Furthermore, the Si $2p$–Si $L_{23}VV$ PEACS directly verifies that the adatom Si $2p$ component (usually denoted by C_3) is correlated with the surface state just below E_F (usually denoted by S_1), which is observed in angle-resolved PES studies.[8,9,24,25]

II. EXPERIMENTAL

An *n*-type Si(111) single-crystal wafer with a resistivity of 0.02 Ω cm was mounted at the end of a sample manipulator, and installed in an ultrahigh vacuum chamber with a base pressure of $\sim 1.5\times10^{-8}$ Pa. A clean reconstructed Si(111)-7×7 surface was prepared by dc heating at >1400 K for several seconds, followed by slow cooling to room temperature (RT) under the pressure of $<3\times10^{-7}$ Pa. A sharp 7×7 pattern was observed with low-energy electron diffraction (LEED). These cleaning procedures were performed once every 6 h to produce clean Si(111)-7×7 between the coincidence measurements.

The sample was irradiated with *p*-polarized SR with an incidence angle of 84° from the surface normal at the beamline 1C of the SR facility in KEK [Photon Factory (PF)]. The photon energy was fixed at 130 eV with a typical energy resolution ($E/\Delta E$) of ~5000. The spot size on the Si surface was ~0.1 mm × 4 mm (vertical×horizontal). For some PEACS measurements the beamline 12A of PF was used. The typical $E/\Delta E$ is ~1000 and the typical spot size on the sample was ~0.5 mm × 5 mm (vertical×horizontal). The contamination and charge-up effects on the sample were checked with LEED and Si $2p$ PES, and were negligible after every measurement.

A homemade coincidence analyzer that can be used for APECS, PEACS, and electron ion coincidence spectroscopy was used for the present experiments [hereafter referred to as an electron electron ion coincidence (EEICO) analyzer].[27] The EEICO analyzer consists of a coaxially symmetric mirror electron energy analyzer (ASMA), a double-pass cylindrical mirror electron energy analyzer (DP-CMA), a time-of-flight ion mass spectrometer (TOF-MS), and so on. The ASMA and the DP-CMA are assembled coaxially and have a common focus. The acceptance angles of the ASMA and the DP-CMA are $59.5^\circ \pm 11.5^\circ$ [solid angle (Ω) = 1.81 sr] and $37.5^\circ \pm 4^\circ$ (Ω = 0.43 sr), respectively. The energy resolution ($E/\Delta E$) of both the ASMA and the DP-CMA is ~55 in the electron kinetic energy range of 20–100 eV.

The procedure for Si $L_{23}VV$ Auger electron Si $2p$ photoelectron coincidence measurements was described in detail previously.[27,28] In short, the Si $2p$ photoelectrons are energy analyzed and detected with the DP-CMA, while Si $L_{23}VV$ Auger electrons are energy analyzed and detected with the ASMA. A multichannel scalar is triggered by the Si $2p$ photoelectrons with a fixed kinetic energy, and the Si $L_{23}VV$ Auger electrons are accumulated as a function of the TOF difference between the Si $2p$ photoelectrons and the Si $L_{23}VV$ Auger electrons. A coincidence signal appears at a specific time region in the APECS TOF spectrum only when the photoelectron and the Auger electron are emitted simultaneously. A series of APECS TOF spectra is acquired by changing the Si $L_{23}VV$ Auger electron kinetic energy (AeKE) at fixed Si $2p$ photoelectron kinetic energy (PeKE). Integrated coincidence signals are plotted as a function of Si $L_{23}VV$ AeKE. We represent this spectrum as Si $L_{23}VV$–Si $2p$ APECS. During the APECS measurement, Si $L_{23}VV$ Auger electron counts detected singly with the ASMA are recorded with a counter simultaneously. The Auger electron counts plotted as a function of Si $L_{23}VV$ AeKE present a conventional AES, which we call the single AES hereafter.

In Si $2p$ photoelectron Si $L_{23}VV$ Auger electron coincidence measurements, on the other hand, the Si $2p$ photoelectrons are detected with the ASMA, while Si $L_{23}VV$ Auger electrons are detected with the DP-CMA. A MCS is triggered by the Si $L_{23}VV$ Auger electrons with a fixed AeKE, and the Si $2p$ photoelectrons are accumulated as a function of the TOF difference between the Si $L_{23}VV$ Auger electrons and the Si $2p$ photoelectrons. Then a series of Si $2p$–Si $L_{23}VV$ PEACS TOF spectra are acquired by changing the PeKE at a fixed AeKE. Integrated coincidence signals plotted as a function of Si $2p$ PeKE present Si $2p$–Si $L_{23}VV$ PEACS. The photoelectron counts measured singly with the ASMA present the single PES.

III. RESULTS AND DISCUSSION

A. Si $L_{23}VV$–Si $2p$ APECS

Figure 1 shows a Si $2p$ PES of clean Si(111)-7×7 at RT measured with the DP-CMA. A similar Si $2p$ PES is obtained with the ASMA (not shown). This spectrum was decomposed into five surface components (C_1, C_2, C_3, C_4, and C_5) and the bulk one (B) by a procedure similar to that in previous works.[8–11] The Lorentzian width of 0.08 eV and Gaussian

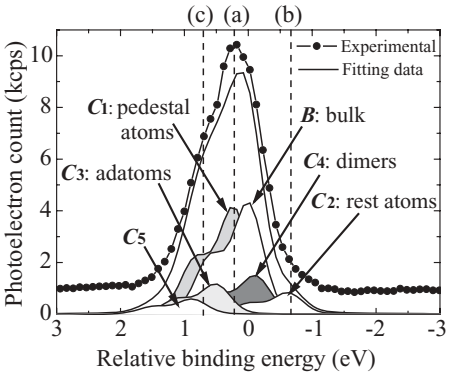

FIG. 1. Si $2p$ photoelectron spectra of clean Si(111)-7×7 at RT on the relative BE scale, where the Si $2p_{3/2}$ bulk peak is taken as the origin, measured with the DP-CMA of the EEICO analyzer. The assignments of the pedestal atoms, the rest atoms, the adatoms, and the dimers are shown. The dashed lines at a relative BE of (a) +0.25, (b) −0.70, and (c) +0.65 eV correspond to the Si $2p$ photoelectrons that were used as the trigger for the Si $L_{23}VV$–Si $2p$ APECS measurements.

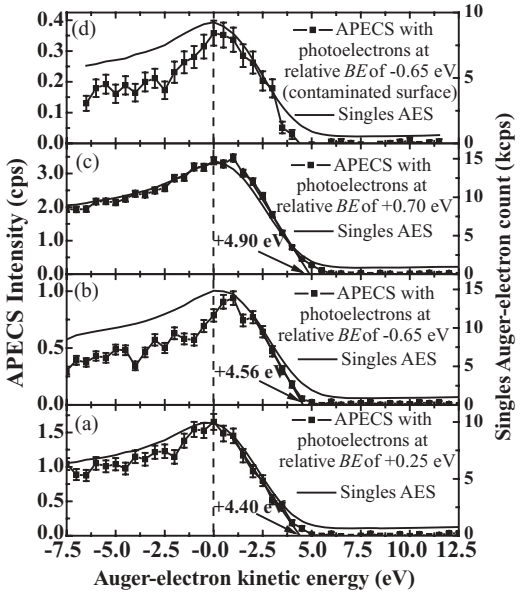

FIG. 2. Si $L_{23}VV$–Si $2p$ APECS of clean Si(111)-7×7 measured in coincidence with Si $2p$ photoelectrons at a relative BE of (a) +0.25, (b) −0.65, and (c) +0.55 eV. (d) The Si $L_{23}VV$–Si $2p$ APECS of Si(111)-7×7 left 12 h without cleaning, measured in coincidence with Si $2p$ photoelectrons at a relative BE of −0.65 eV. The cumulative time per datum was (a) 600, (b) 1200, (c) 1200, and (d) 900 s, respectively. APECS are drawn on the relative AeKE scale, where the maximum peak of single AES (AeKE ≅ 87.5 ± 1.7 eV) is taken as the origin. The lines obtained by least-squares linear fitting in the maximum-peak-tail region with 20%–80% intensity are also shown.

width of 0.38–0.48 eV are used for the Si $2p$ PES peak fitting. The spin-orbit coupling between Si $2p_{1/2}$ and Si $2p_{3/2}$ and the intensity ratio of Si $2p_{1/2}$ to Si $2p_{3/2}$ (Si $2p_{1/2}$/Si $2p_{3/2}$) are taken as 0.6 eV and 0.5, respectively. The fitting curves well reproduced the measured Si $2p$ PES. The relative binding energy (BE) shifts of the Si $2p_{3/2}$ peak of the C_1, C_2, C_3, C_4, and C_5 components to the bulk Si $2p_{3/2}$ peak are +0.25, −0.65, +0.53, −0.1, and +0.90 eV, respectively. These values are in good agreement with those reported in previous works.[8,9] Karlsson *et al.* assigned the C_1, C_2, C_3, and C_4 components to the pedestal atoms, the rest atoms, the adatoms, and the dimers, respectively.[8] Other research groups agreed on the main conclusions that the rest atoms are responsible for the component C_2 shifted to lower binding energies and that the adatom component C_3 is shifted toward higher binding energies compared to the bulk component.[10,11] The dashed vertical lines at (a) +0.25, (b) −0.65, and (c) +0.70 eV indicate the kinetic energy of Si $2p$ photoelectrons used as the trigger for the Si $L_{23}VV$–Si $2p$ APECS measurements (see below).

Figures 2(a)–2(c) show enlarged Si $L_{23}VV$–Si $2p$ APECS of clean Si(111)-7×7 measured in coincidence with Si $2p$ photoelectrons at the relative BE of (a) +0.25, (b) −0.65, and (c) +0.70 eV corresponding to the Si $2p_{3/2}$ photoelectron of the pedestal atoms, Si $2p_{3/2}$ photoelectron of the rest atoms, and Si $2p_{3/2,1/2}$ photoelectron of the pedestal atoms, respectively. Figure 2(d) shows a Si $L_{23}VV$–Si $2p$ APECS of Si(111)-7×7 at 12 h after the Si cleaning procedure, measured in coincidence with Si $2p_{3/2}$ photoelectrons at a relative BE of −0.65 eV. This surface is thought to be contaminated with residual gases. These Si $L_{23}VV$–Si $2p$ APECS are drawn on the relative AeKE scale, where the maximum peak of single AES (AeKE ≅ 87.5 ± 1.7 eV) is taken as the origin. Note that APECS signals are almost negligible in the relative AeKE regions of >+5 eV, where valence photoelectron peaks appear in conventional SR-PES. The IMFP of Si $2p$ photoelectrons from the Si surface at $h\nu = 130$ eV was reported to be ∼3.3 Å.[29] Based on the empirical formulation by Tanuma, Penn, and Powell (TPP-2 equation),[30] the IMFP of Si $L_{23}VV$ Auger electrons with a KE of 90 eV in the Si solid state is estimated to be ∼5.1 Å. The ED_{APECS} is calculated to be ∼1.3 Å using Eq. (1) under this condition. This value is shorter than the averaged thickness of a monolayer of Si(111) (∼1.57 Å). Thus the bulk component is substantially suppressed while the surface ones are enhanced in APECS. Therefore, the Si $L_{23}VV$–Si $2p$ APECS measured in coincidence with Si $2p$ photoelectrons at a relative BE of +0.25 eV [Fig. 2(a)] can be attributed mainly to the Si L_3VV AES of the pedestal atoms. The Si $L_{23}VV$–Si-$2p$ APECS measured in coincidence with the Si $2p$ photoelectrons at a relative BE of −0.65 eV [Fig. 2(b)] can be attributed predominantly to the Si L_3VV AES of the rest atoms, while the Si $L_{23}VV$–Si $2p$ APECS measured in coincidence with photoelectrons at a relative BE of +0.7 eV [Fig. 2(c)] can be attributed mainly to the Si $L_{23}VV$ AES of the pedestal atoms. The width of the APECS in Fig. 2(a) is slightly narrower than that in Fig. 2(c), supporting the conjecture that the APECS in Fig. 2(a) is mainly composed of Si L_3VV AES of the pedestal atoms. The width of the APECS in Fig. 2(b) is much narrower than those of the other APECS, indicating the high purity of the Si L_3VV AES component of the rest atoms. The highest peak of the Si $L_{23}VV$–Si $2p$ APECS of the rest atoms is shifted by ∼1 eV to the higher AeKE side in comparison with that of the other APECS and single AES. The width of APECS in Fig. 2(d) is much broader than that of Fig. 2(b), suggesting that the rest atoms are contaminated with residual gases after 12 h without cleaning. This result is consistent with a STM

study that reported that the rest atoms are more reactive than adatoms.[4] These fundamental spectroscopic data are useful for Si surface analysis using AES. The APECS can be used as not only elemental but also chemical environmental fingerprints.

As stated in Sec. I, the AeKE of the highest peak ($\mathrm{AeKE_{HP}}$) in Si $L_{23}VV$–Si 2p APECS provides information on the BE of the valence band at the highest DOS (BE_{VH}) associated with the surface site taken as the trigger.[18] The AeKE in a Si $L_{23}VV$ peak is generally given by the following equation:[18]

$$\mathrm{AeKE}_{L_{23}VV} = \mathrm{BE}_{L_{23}} - \mathrm{BE}_{V_1} - \mathrm{BE}_{V_2} - H + R - \phi, \quad (3)$$

where $\mathrm{BE}_{L_{23}}$, BE_{V_1}, and BE_{V_2} denote the binding energies of Si L_{23} and the valence electrons. H is the hole-hole interaction energy, R is the relaxation energy, and ϕ is the work function of the electron analyzer. Assuming that the $(-H + R)$ term does not depend on the Si site, the difference in BE_{VH} between two surface sites ($\mathrm{BE}^{\mathrm{S1}}_{VH} - \mathrm{BE}^{\mathrm{S2}}_{VH}$) is approximately given by

$$\mathrm{BE}^{\mathrm{S1}}_{VH} - \mathrm{BE}^{\mathrm{S2}}_{VH} = \tfrac{1}{2}\left[\left(\mathrm{BE}^{\mathrm{S1}}_{2p} - \mathrm{BE}^{\mathrm{S2}}_{2p}\right) - \left(\mathrm{AeKE}^{\mathrm{S1}}_{\mathrm{HP}} - \mathrm{AeKE}^{\mathrm{S2}}_{\mathrm{HP}}\right)\right], \quad (4)$$

where the superscripts S1 and S2 denote the two specific surface sites.[18] $\mathrm{BE}^{\mathrm{S1}}_{2p}$ and $\mathrm{BE}^{\mathrm{S2}}_{2p}$ can be estimated from Si 2p PES (see Fig. 1), while $\mathrm{AeKE}^{\mathrm{S1}}_{\mathrm{HP}}$ and $\mathrm{AeKE}^{\mathrm{S2}}_{\mathrm{HP}}$ are obtained from the surface-site-selective Si $L_{23}VV$–Si 2p APECS (see Fig. 2). ($\mathrm{BE}^{\text{rest atoms}}_{VH} - \mathrm{BE}^{\text{pedestal atoms}}_{VH}$) is estimated to be approximately -0.95 eV using Eq. (4). This value is consistent with the difference in BE_{2p} between the rest atoms and the pedestal atoms ($\mathrm{BE}^{\text{rest atoms}}_{2p} - \mathrm{BE}^{\text{pedestal atoms}}_{2p} \approx -0.90$ eV). In an angle-resolved PES study of Si(111)-7×7, Uhrberg *et al.* found three surface states at ∼0.2 (S_1), ∼0.8 (S_2), and ∼1.8 eV (S_3) below E_{F}.[24] First-principles calculations[26] and a CITS study[3] ascribed them to the adatom dangling bonds, the rest-atom dangling bonds, and the adatom back bonds, respectively. Therefore, $\mathrm{BE}^{\text{rest atoms}}_{VH}$ and $\mathrm{BE}^{\text{pedestal atoms}}_{VH}$ are thought to be ∼0.8 and ∼1.8 eV because pedestal atoms are bonded to the adatoms. The binding energy difference ($\mathrm{BE}^{\text{rest atoms}}_{VH} - \mathrm{BE}^{\text{pedestal atoms}}_{VH} \approx -1.0$ eV) is very close to the value obtained in the present APECS study.

The cutoff energy of Si $L_{23}VV$–Si 2p APECS in the high AeKE side, on the other hand, provides information of the BE of the valence-band maximum ($\mathrm{BE_{VBM}}$) associated with the surface site taken as the trigger.[18] Here, we defined the AeKE of the cutoff ($\mathrm{AeKE_{cutoff}}$) as the intersection point of the x axis and the line obtained from least-squares linear line fitting in the maximum-peak-tail region with 20%–80% intensity. The $\mathrm{AeKE_{cutoff}}$ of Si L_3VV AES for the rest atoms and the pedestal atoms is estimated to be +4.56 and +4.40 eV on the relative AeKE scale, respectively (see Fig. 2). Assuming that the hole-hole interaction energy and the relaxation energy do not depend on the Si site, the $\mathrm{BE_{VBM}}$ difference between two specific surface sites ($\mathrm{BE}^{\mathrm{S1}}_{\mathrm{VBM}} - \mathrm{BE}^{\mathrm{S2}}_{\mathrm{VBM}}$) can be estimated by

$$\mathrm{BE}^{\mathrm{S1}}_{\mathrm{VBM}} - \mathrm{BE}^{\mathrm{S2}}_{\mathrm{VBM}} = \tfrac{1}{2}\left[\left(\mathrm{BE}^{\mathrm{S1}}_{2p} - \mathrm{BE}^{\mathrm{S2}}_{2p}\right) - \left(\mathrm{AeKE}^{\mathrm{S1}}_{\mathrm{cutoff}} - \mathrm{AeKE}^{\mathrm{S2}}_{\mathrm{cutoff}}\right)\right], \quad (5)$$

where ($\mathrm{BE}^{\mathrm{S1}}_{2p} - \mathrm{BE}^{\mathrm{S2}}_{2p}$) can be estimated from Si 2p PES (see Fig. 1), while ($\mathrm{AeKE}^{\mathrm{S1}}_{\mathrm{cutoff}} - \mathrm{AeKE}^{\mathrm{S2}}_{\mathrm{cutoff}}$) is given by the Si $L_{23}VV$–Si 2p APECS of the specific surface sites (see Fig. 2).[18] ($\mathrm{BE}^{\text{rest atoms}}_{\mathrm{VBM}} - \mathrm{BE}^{\text{pedestal atoms}}_{\mathrm{VBM}}$) is estimated to be ∼−0.53 eV. This result indicates that the VBM of the rest atoms is shifted by 0.53 eV toward E_{F}, relative to that in the vicinity of the pedestal atoms.

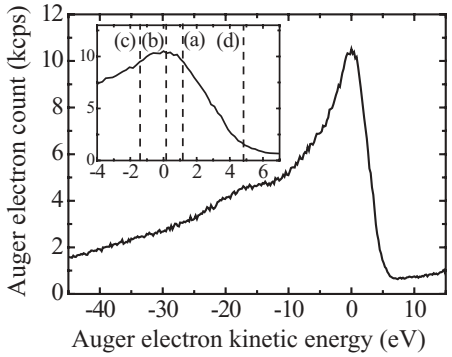

FIG. 3. Si $L_{23}VV$ AES of clean Si(111)-7×7 at RT on the relative AeKE scale, where the maximum peak position of the conventional AES is taken as the origin, measured with the DP-CMA of the EEICO analyzer. An expanded spectrum is also shown. The dashed lines at a relative AeKE of (a) +1.1, (b) +0.1, (c) −1.4, and (d) +4.8 eV correspond to the Si $L_{23}VV$ Auger electrons that were used as the trigger for the Si 2p–Si $L_{23}VV$ PEACS measurements.

B. Si 2p–Si $L_{23}VV$ PEACS

Figure 3 shows a conventional Si $L_{23}VV$ AES of Si(111)-7×7 at RT measured with the DP-CMA of the EEICO analyzer. A similar spectrum is obtained with the ASMA (not shown). The dashed lines (a)–(d) in the inserted figure indicate the kinetic energies of Auger electrons that were used as the trigger for the Si 2p–Si $L_{23}VV$ PEACS measurements (see below). Figures 4(a)–4(c) show Si 2p photoelectron Si $L_{23}VV$ Auger electron coincidence spectra (Si 2p–Si $L_{23}VV$ PEACS) of clean Si(111)-7×7 (filled circles), measured in coincidence with Si $L_{23}VV$ Auger electrons at the relative AeKE of (a) +1.1, (b) +0.1, and (c) −1.4 eV (see Fig. 3). The solid lines with open circles in Figs. 4(a)–4(c) are single Si 2p PES measured simultaneously with each Si 2p–Si $L_{23}VV$ PEACS. The Si $2p_{3/2}$ bulk peak of the single PES measured with the ASMA is taken as the origin of the relative BE. Note that PEACS signals are negligible in the relative BE regions of $>+1.75$ and <-1.25 eV, where the tail of Auger electron peaks and secondary electrons appear in conventional SR-CL-PES (see Fig. 1). $\mathrm{ED_{PEACS}}$ obtained from Eq. (1) is calculated to be ∼1.2 Å under this measurement condition. $\mathrm{ED_{PEACS}}$ is also shorter than the averaged thickness of a monolayer of Si(111). Therefore the Si 2p components of the topmost-surface atoms (the adatoms and the rest atoms) are expected to be enhanced in Si 2p–Si $L_{23}VV$ PEACS. Note that PEACS can probe the topmost-surface atoms located in relatively depressed areas such as rest atoms in Si(111)-7×7, in contrast to STM and STS.

The Si 2p–Si $L_{23}VV$ PEACS in Fig. 4 are fitted with each Si 2p component obtained in the deconvolution of the Si 2p PES shown in Fig. 1. The spectral weights of individual Si 2p components in single PES and Si 2p–Si $L_{23}VV$ PEACS are summarized in Table I. In every PEACS, the spectral weight of the bulk component is considerably reduced from 38%

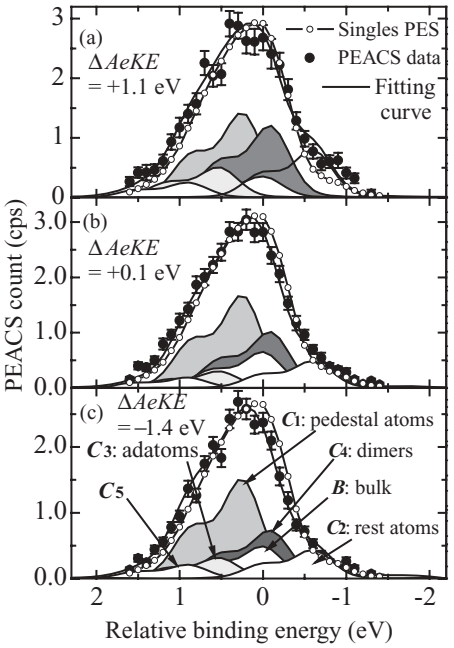

FIG. 4. Si 2*p*–Si $L_{23}VV$ PEACS of clean Si(111)-7×7 measured in coincidence with a relative AeKE at (a) +1.1, (b) +0.1, and (c) −1.4 eV are represented by filled circles. The black solid line with open circles is the single PES measured simultaneously with each PEACS. The Si 2*p*–Si $L_{23}VV$ PEACS are fitted with each Si 2*p* component obtained by the deconvolution of the Si 2*p* PES shown in Fig. 1. The fitting spectra are represented by the solid lines. The Si $2p_{3/2}$ bulk peak of the single PES measured with the ASMA was taken as the origin of the relative PeKE. The cumulative time per datum in (a)–(d) is 600 s.

to 8%–13%, demonstrating the topmost-surface selectivity of PEACS. The spectral weights of the dimers and the rest atoms, on the other hand, are considerably increased from 7% to 20%–26%, and from 5% to 11%–17%, respectively. The variations of the spectral weights of the adatoms and the pedestal atoms are relatively small.

It is well known that the adatoms are positively charged because the surface state composed of the adatom dangling bonds (usually denoted by S_1) is partially filled.[3,24–26] Recent x-ray and high-energy electron diffraction studies concluded that the charge transfer from each adatom site to the underlying layers is $0.26 \pm 0.04e^{\hbar}$.[31] This electronic structure seems to be the reason why the spectral weights of the adatoms are scarcely increased in the Si 2*p*–Si $L_{23}VV$ PEACS at a relative AeKE of +1.1, +0.1, and −1.4 eV (see Fig. 4 and Table I). The adatom dangling bond state is expected to mainly contribute to Si $L_{23}VV$ AES at a relative AeKE of $>+1.1$ eV, while the other adatom-related valence bands form AES peaks at a relative AeKE of <-1.4 eV, because the binding energy of the other bands shifts to the larger side owing to the positive charge at the adatoms.[32]

PEACS provide information on the charge state of other surface sites. As discussed in the previous section on APECS, the difference in BE_{VH} between a surface site and bulk (BE^{S}_{VH} and BE^{B}_{VH}) is approximately given by

$$\mathrm{BE}^{S}_{VH} - \mathrm{BE}^{B}_{VH} = \tfrac{1}{2}\left[\left(\mathrm{BE}^{S}_{2p} - \mathrm{BE}^{B}_{2p}\right) - \left(\mathrm{AeKE}^{S}_{\mathrm{HP}} - \mathrm{AeKE}^{B}_{\mathrm{HP}}\right)\right], \quad (6)$$

where the superscripts *S* and *B* denote the surface and the bulk sites. In terms of the initial-state effect,

$$\mathrm{BE}^{S}_{VH}\ (\text{positively charged site}) > \mathrm{BE}^{B}_{VH} > \mathrm{BE}^{S}_{VH}\ (\text{negatively charged site}) \quad (7)$$

is expected,[32] when the related valence bands are filled. In the PEACS measured at the relative AeKE of +1.1, +0.1, and −1.4 eV, the order of increment of the spectral weight ($\Delta\mathrm{SW}_{\text{rel AeKE}=+1.1\text{ eV}}$, $\Delta\mathrm{SW}_{\text{rel AeKE}=+0.1\text{ eV}}$, and $\Delta\mathrm{SW}_{\text{rel AeKE}=-1.4\text{ eV}}$ is $\Delta\mathrm{SW}_{\text{rel AeKE}=+1.1\text{ eV}} < \Delta\mathrm{SW}_{\text{rel AeKE}=+0.1\text{ eV}} < \Delta\mathrm{SW}_{\text{rel AeKE}=-1.4\text{ eV}}$ for the pedestal atoms, and $\Delta\mathrm{SW}_{\text{rel AeKE}=+1.1\text{ eV}} > \Delta\mathrm{SW}_{\text{rel AeKE}=+0.1\text{ eV}} \geqslant \Delta\mathrm{SW}_{\text{rel AeKE}=-1.4\text{ eV}}$ for the dimers and the rest atoms as shown in Table I. These results suggest that $\mathrm{BE}^{\text{pedestal}}_{VH} > \mathrm{BE}^{B}_{VH} > BE^{\text{dimers}}_{VH}, BE^{\text{rest atoms}}_{VH}$. Because the valence bands related with the dimers, the rest atoms, and the pedestal atoms are filled,[26] the present results suggest that the dimers and the rest atoms are negatively charged while the pedestal atoms are positively charged. These results are consistent with previous SR-CL-PES studies in terms of the initial-state effect.[8–11]

TABLE I. The spectral weights contributed by individual Si 2*p* components in the single Si 2*p* PES in Fig. 1 and each Si 2*p*–Si $L_{23}VV$ PEACS of Si(111)-7×7 in Figs. 4(a)–4(c) and Fig. 5. The increment and decrement of the spectral weight of individual components are also shown.

	C_5	C_3	C_1	B	C_4	C_2
Relative BE (eV)	+0.90	+0.53	+0.25	0	−0.10	−0.65
Assignments by Karlsson *et al.* (Ref. 8)		Adatoms	Pedestal atoms	Bulk	Dimers	Rest atoms
Single Si 2*p* PES	7%	8%	35%	38%	7%	5%
Fig. 4(a)	6% (−1%)	12% (+4%)	31% (−4%)	8% (−30%)	26% (+19%)	17% (+12%)
Relative AeKE = +1.1 eV						
Fig. 4(b)	5% (−2%)	7% (−1%)	40% (+5%)	13% (−25%)	24% (+17%)	11% (+6%)
Relative AeKE = +0.1 eV						
Fig. 4(c)	6% (−1%)	9% (+1%)	41% (+6%)	13% (−25%)	20% (+13%)	11% (+6%)
Relative AeKE = −1.4 eV						
Fig. 5	13% (+6%)	30% (+22%)	17% (−18%)	18% (−20%)	10% (+3%)	12% (+7%)
Relative AeKE = +4.8 eV						

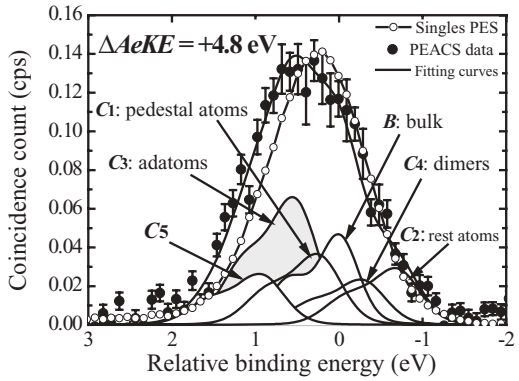

FIG. 5. Si 2*p*–Si $L_{23}VV$ PEACS of clean Si(111)-7×7 measured in coincidence with a relative AeKE at +4.8 eV are represented by filled circles. The black solid line with open circles is the single PES measured simultaneously with PEACS. The Si 2*p*–Si $L_{23}VV$ PEACS is fitted by a procedure similar to that in previous SR-CL-PES works. The fitting spectra are represented by the solid lines. The Si $2p_{3/2}$ bulk peak of the single PES measured with the ASMA is taken as the origin of the relative PeKE. The cumulative time per datum is 30 min.

As described above, the adatoms are positively charged because the surface state (S_1) composed of the adatom dangling bonds is partially filled and pins E_F.[3,8,9,24–26] This is the reason why the adatom component C_3 is shifted toward higher binding energies compared to the bulk component.[8–11] To verify the correlation between the valence surface state S_1 and Si 2*p* adatom component C_3, we measured Si 2*p*–Si $L_{23}VV$ PEACS taking Auger electrons at a relative AeKE of +4.8 eV as the trigger (Fig. 5). The relative AeKE of +4.8 eV corresponds to the Auger processes that involve valence electrons in the surface state S_1 just below E_F. The resolution is slightly poorer than the spectra shown in Fig. 4 because beamline 12A at PF was used for this measurement. The curve fitting of the PEACS shows that the Si 2*p* adatom component C_3 is greatly enhanced. The spectral weight contributed by C_3 in the Si 2*p*–Si $L_{23}VV$ PEACS is ∼30% (Table I). This value is approximately three times larger than that of C_3 in the Si 2*p* PES. This is direct evidence that the Si 2*p* component C_3 is correlated with the adatom dangling bond state (S_1).

IV. CONCLUSIONS

Using an EEICO analyzer with a high resolution and a high sensitivity, we have successfully measured Si $L_{23}VV$–Si 2*p* APECS and Si 2*p*–Si $L_{23}VV$ PEACS of clean Si(111)-7×7. The escape depth of the APECS and PEACS is estimated to be ∼1.3 and ∼1.2 Å, which are shorter than the averaged thickness of a monolayer of Si(111).

APECS provides fundamental spectroscopic data that are useful for surface analysis using AES. The Si $L_{23}VV$–Si 2*p* APECS measured in coincidence with Si $2p_{3/2}$ photoelectrons emitted from the rest atoms and the pedestal atoms showed that the position where the highest DOS of the valence band located in the vicinity of the rest atoms is shifted 0.95 eV to E_F relative to that in the vicinity of the pedestal atoms. Meanwhile, the valence-band maximum located in the vicinity of the rest atoms was shown to be shifted 0.53 eV to E_F relative to that in the vicinity of the pedestal atoms.

In Si 2*p*–Si $L_{23}VV$ PEACS the bulk component is considerably suppressed while components of the topmost-surface atoms are enhanced. Furthermore, Si 2*p*–Si $L_{23}VV$ PEACS measured at a relative AeKE of +1.1, +0.1, and −1.4 eV showed that the dimers and the rest atoms are negatively charged while the pedestal atoms are positively charged. PEACS can be used to identify not only the topmost-surface components but also negatively or positively charged components. The Si 2*p*–Si $L_{23}VV$ PEACS measured in coincidence with a relative AeKE of +4.8 eV provided direct evidence for the correlation of the Si 2*p* component C_3 and the adatom dangling bonding surface state S_1.

ACKNOWLEDGMENTS

We express our sincere thanks to the members of the Photon Factory for their valuable help during the course of the experiments. This work was partly supported by PRESTO (Structure Function and Measurement Analysis) from the Japan Science and Technology Agency (JST). This work was performed with the approval of the Photon Factory Program Advisory Committee (PF PAC Nos. 2006S2-002 and 2009G222).

[1] K. Takayanagi, Y. Tanishiro, M. Takahashi, and S. Takahashi, J. Vac. Sci. Technol. A **3**, 1502 (1985).
[2] G. Binnig, H. Rohrer, Ch. Gerber, and E. Weibel, Phys. Rev. Lett. **50**, 120 (1983).
[3] R. J. Hamers, R. M. Tromp, and J. E. Demuth, Phys. Rev. Lett. **56**, 1972 (1986).
[4] R. Wolkow and Ph. Avouris, Phys. Rev. Lett. **60**, 1049 (1988).
[5] L. Chen, B. C. Pan, H. Xiang, B. Wang, J. Yang, J. G. Hou, and Q. Zhu, Phys. Rev. B **75**, 085329 (2007).
[6] M. Hupalo, C. Z. Wang, B. J. Min, K. M. Ho, and M. C. Tringides, Phys. Rev. B **67**, 115333 (2003).
[7] Y. L. Wang, H.-J. Gao, H. M. Guo, H. W. Liu, I. G. Batyrev, W. E. McMahon, and S. B. Zhang, Phys. Rev. B **70**, 073312 (2004).
[8] C. J. Karlsson, E. Landemark, Y.-C. Chao, and R. I. G. Uhrberg, Phys. Rev. B **50**, 5767 (1994).
[9] R. I. G. Uhrberg, T. Kaurila, and Y.-C. Chao, Phys. Rev. B **58**, R1730 (1998).
[10] G. LeLay, M. Göthelid, T. M. Grekh, M. Björkquist, U. O. Karlsson, and V. Yu. Aristov, Phys. Rev. B **50**, 14277 (1994).
[11] J. J. Paggel, W. Theis, K. Horn, Ch. Jung, C. Hellwig, and H. Petersen, Phys. Rev. B **50**, 18686 (1994).
[12] H. W. Haak, G. A. Sawatzky, and T. D. Thomas, Phys. Rev. Lett. **41**, 1825 (1978).
[13] G. A. Sawatzky, in *Auger Electron Spectroscopy*, edited by C. L. Briant and R. P. Messer (Academic, San Diego, CA, 1988) Chap. 5, pp. 167–243.

[14]*Correlation Spectroscopy of Surfaces, Thin Films, and Nanostructures*, edited by J. Berakdar and J. Kirschner (Wiley-VCH, Weinheim, Germany, 2004).
[15]G. van Riessen, Z. Wei, R. S. Dhaka, C. Winkler, F. O. Schumann, and J. Kirschner, J. Phys. Condens. Matter **22**, 092201 (2010).
[16]E. Jensen, R. A. Bartynski, M. Weinert, S. L. Hulbert, E. D. Johnson, and R. F. Garrett, Phys. Rev. B **41**, 12468 (1990).
[17]R. A. Bartynski, S. Yang, S. L. Hulbert, C.-C. Kao, M. Weinert, and D. M. Zehner, Phys. Rev. Lett. **68**, 2247 (1992).
[18]T. Kakiuchi, S. Hashimoto, N. Fujita, M. Tanaka, K. Mase, and S. Nagaoka, J. Phys. Soc. Jpn. **79**, 064714 (2010).
[19]G. L. Lay, Mater. Chem. Phys. **40**, 212 (1995).
[20]M. V. Gomoyunova and I. I. Pronin, Tech. Phys. **49**, 1249 (2004).
[21]W. S. M. Werner, W. Smekal, H. Störi, H. Winter, G. Stefani, A. Ruocco, F. Offi, R. Gotter, A. Morgante, and F. Tommasini, Phys. Rev. Lett. **94**, 038302 (2005).
[22]G. Stefani, S. Iacobucci, A. Ruocco, and R. Gotter, J. Electron Spectrosc. Relat. Phenom. **127**, 1 (2002).
[23]T. Kakiuchi, S. Hashimoto, N. Fujita, M. Tanaka, K. Mase, and S. Nagaoka, Surf. Sci. **604**, L27 (2010).
[24]R. I. G. Uhrberg, G. V. Hansson, J. M. Nicholls, P. E. S. Persson, and S. A. Flodström, Phys. Rev. B **31**, 3805 (1985).
[25]R. Losio, K. N. Altmann, and F. J. Himpsel, Phys. Rev. B **61**, 10845 (2000).
[26]J. E. Northrup, Phys. Rev. Lett. **57**, 154 (1986).
[27]T. Kakiuchi, S. Hashimoto, N. Fujita, K. Mase, M. Tanaka, and M. Okusawa, J. Vac. Soc. Jpn. **51**, 749 (2008) (in Japanese).
[28]T. Kakiuchi, E. Kobayashi, N. Okada, K. Oyamada, M. Okusawa, K. K. Okudaira, and K. Mase, J. Electron Spectrosc. Relat. Phenom. **161**, 164 (2007).
[29]F. J. Himpsel, F. R. McFeely, A. Taleb-Ibrahimi, J. A. Yarmoff, and G. Hollinger, Phys. Rev. B **38**, 6084 (1988).
[30]S. Tanuma, C. J. Powell, and D. R. Penn, Surf. Interface Anal. **17**, 911 (1991).
[31]J. Ciston, A. Subramanian, I. K. Robinson, and L. D. Marks, Phys. Rev. B **79**, 193302 (2009).
[32]N. Mårtensson and A. Nilsson, J. Electron Spectrosc. Relat. Phenom. **75**, 209 (1995).